

<b>REPORT DOCUMENTATION PAGE</b>				<b>Form Approved</b> <b>OMB No. 0704-0188</b>	
<small>Public reporting burden for this collection of information is estimated to average 1 hour per response, including the time for reviewing instructions, searching data sources, gathering and maintaining the data needed, and completing and reviewing the collection of information. Send comments regarding this burden estimate or any other aspect of this collection of information, including suggestions for reducing this burden to Washington Headquarters Service, Directorate for Information Operations and Reports, 1215 Jefferson Davis Highway, Suite 1204, Arlington, VA 22202-4302, and to the Office of Management and Budget, Paperwork Reduction Project (0704-0188) Washington, DC 20503.</small>					
<b>PLEASE DO NOT RETURN YOUR FORM TO THE ABOVE ADDRESS.</b>					
<b>1. REPORT DATE (DD-MM-YYYY)</b> 1/11/06		<b>2. REPORT TYPE</b> Final		<b>3. DATES COVERED (From - To)</b> 2/1/04-7/31/05	
<b>4. TITLE AND SUBTITLE</b> Narrow Linewidth Tunable Solid-State Microchip Lasers for Precision Inertial Navigation Systems (PINS)				<b>5a. CONTRACT NUMBER</b> W911NF-04-1-0034	
				<b>5b. GRANT NUMBER</b> 	
				<b>5c. PROGRAM ELEMENT NUMBER</b> 	
<b>6. AUTHOR(S)</b> Prof. Franz X. Kaertner				<b>5d. PROJECT NUMBER</b> 	
				<b>5e. TASK NUMBER</b> 	
				<b>5f. WORK UNIT NUMBER</b> 	
<b>7. PERFORMING ORGANIZATION NAME(S) AND ADDRESS(ES)</b> Massachusetts Institute of Technology 77 Massachusetts Avenue Cambridge, MA 02139-4307				<b>8. PERFORMING ORGANIZATION REPORT NUMBER</b> 	
<b>9. SPONSORING/MONITORING AGENCY NAME(S) AND ADDRESS(ES)</b> U.S. Army Research Office 4300 South Miami Boulevard Research Triangle Park, NC 27707-2211				<b>10. SPONSOR/MONITOR'S ACRONYM(S)</b> 	
				<b>11. SPONSORING/MONITORING AGENCY REPORT NUMBER</b> 4 5 5 9 8 . 1 - P H - D R P	
<b>12. DISTRIBUTION AVAILABILITY STATEMENT</b> Approved for Public Release; Distribution Unlimited.					
<b>13. SUPPLEMENTARY NOTES</b>					
<b>14. ABSTRACT</b> In Phase I of the PINS program we where able to demonstrate a multimode operating Cr:LiCAF miniaturized laser generating up to 300 mW of output power. In addition we developed a filter that enables tuning over 0.9nm and single-mode operation. Initial demonstrations with test devices showed single-mode operation up to 20mW of output power with linewidth on the order 5MHz. We are confident, that further development could bring the single mode output power beyond 150mW and the linewidth well below the 100kHz level and with additional effort into the Hz range. We have also demonstrated significant index changes in GaP wafers by carrier injection, which can be used later for fast phase modulation in the laser potentially with GHz modulation speed.					
<b>15. SUBJECT TERMS</b>					
<b>16. SECURITY CLASSIFICATION OF:</b>			<b>17. LIMITATION OF ABSTRACT</b>	<b>18. NUMBER OF PAGES</b> 29	<b>19a. NAME OF RESPONSIBLE PERSON</b> Franz X. Kaertner
a. REPORT	b. ABSTRACT	c. THIS PAGE			<b>19b. TELEPHONE NUMBER (Include area code)</b> 617-452-3616

## **Final Report**

# **Narrow Linewidth Tunable Solid-State Microchip Lasers for Precision Inertial Navigation Systems (PINS)**

**February 1, 2004 to July 31, 2005**

**F. X. Kärtner**

Department of Electrical Engineering and Computer Science  
and Research Laboratory of Electronics,  
Massachusetts Institute of Technology, Cambridge MA 02319

## **Outline**

### **A. Introduction**

### **B. Device Concepts**

B.1 – Overview of final device concept

B.2 – Cavity configurations

B.3 – Semiconductor device for tuning, frequency modulation and locking

### **C. Multimode operation**

C.1 – Optimized output performance

C.2 – Cavity losses

### **D. Single mode operation**

D.1 – Initial version

D.2 – Filter design and characterization

D.3 – Single mode operation

i. Few mode output power

ii. Improved mechanical design

iii. Single mode linewidth measurements and noise spectrum

D.4 – Filter tunability: progress made in Ti:SAF

D.5 – Tuning and modulation by carrier injection in semiconductors

D.6 – Conclusion or why did we miss to deliver the Phase I milestones on time?

### **E. Future possible work**

E.1 – Increasing the output power and packaging

E.2 – Graded filter for widely tunable single-frequency laser

E.3 – Optimized mechanical design

E.5 – Compact ULE-cavities for Hertz-linewidth lasers

### **F. References**

## **A. Introduction**

The successful implementation of Precision Inertial Navigation Systems (PINS) based on atom interferometry requires compact, tunable, single frequency laser sources that have narrow linewidths at 780 and 850nm and provide greater than 100mW of output power for Rubidium and Cesium atomic traps. The laser linewidth should be less than 100kHz and for locking to ULE-cavities linewidths as narrow as 100Hz to 1kHz would be desirable. The laser also needs to be tunable over a plus/minus 150 MHz range within 10 microseconds and tunable over 2nm at slower speed to satisfy the applications intended in the PINS program. Cr:LiCAF laser material with its long upper state lifetime is ideal candidate material to be used in a single frequency to meet the PINS project requirements.

In Phase I of the PINS program we were able to demonstrate a multimode operating Cr:LiCAF microchip laser generating up to 300 mW of output power. In addition we developed a filter that enables tuning over 0.9nm and single-mode operation. Initial demonstrations with test devices showed single-mode operation up to 20mW of output power with linewidth on the order 5MHz. We are confident, that further development could bring the single mode output power beyond 150mW and the linewidth well below the 100kHz level and with additional effort into the Hz range. We have also demonstrated significant index changes in GaP wafers by carrier injection, which can be used later for fast phase modulation in the laser potentially with GHz modulation speed.

## **B. Device Concepts**



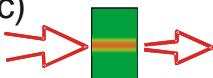
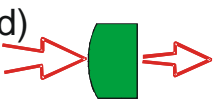
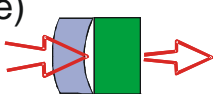
Diode-pumped solid-state lasers in microchip or monolithic form such as Non-Planar Ring oscillators are known for several desirable properties including intrinsic low noise behavior due to the long upperstate lifetime of solid-state laser materials [1], good pointing stability, and large average power capability. Consequently we have pursued the construction of the tunable single-frequency mini laser presented in this report. In this section we present an overview of the laser design including the cavity design, the single frequency selection mechanism, and the semiconductor phase modulation concept for fast

tuning. In later sections we present the experimental results and in particular we present the promising results of 300mW output power with a 37mW threshold for multimode operation, and 20mW single mode operation with a 5MHz linewidth.

### **B.1 – Cavity configurations**

In Phase I of this program we investigated how to exploit the highest possible doping for the Cr:LICAF crystal, together with its high upperstate lifetime quenching temperature of 250°C, to construct very short-cavity microchip and mini-lasers of only 2mm length in order to enable simple single-frequency operation due to the large longitudinal mode spacing. Such short lasers have already a free spectral range (FSR) of about 0.1 nm corresponding to 50 GHz. Figure B1. shows the cavity geometries investigated by simulations and experimentally.

Figure B1 a and b indicate the formation of a stable cavity mode in a flat/flat Cr:LICAF crystal due to the thermally induced gaussian duct or the bowing of the cavity surfaces due to the heat deposition in the crystal via the pump beam. Unfortunately, or fortunately (see discussion in section E.1), these two effects balance each other and therefore these effects can not be used to form a stable microchip cavity as is the case in many other microchip lasers. Also gain guiding, as observed in high gain Nd:YVO4 lasers [7], is too weak in the Cr:LICAF laser to form a stable mode. Therefore, we decided to explore the options shown in Fig. B1 (d) and (e), i.e. to form a stable cavity mode by either a curved surface on the crystal or an external curved mirror and a flat/flat crystal properly coated with and output coupler on one side and an AR-coating on the side facing the curved mirror. It turned out, that polishing of the soft Cr:LICAF crystals with a strong curvature was a non-trivial task and the company we charged with this task could not deliver the promised quality of polishing and coating. For this and other reasons that are discussed later the most promising setup turned out to be the plano-convex option Fig. B1 (e).

a)		thermal lens	✗	$dn/dT < 0$
b)		thermal expansion	✗	canceled out by $dn/dT < 0$
c)		gain guiding	✗	gain is too small to overcome $dn/dT < 0$
d)		plano-convex crystal	✓	
e)		composite cavity	✓	

**Figure B.1:** Different cavity configurations investigated for construction of a Cr:LICAF mini- or microchip laser.

## B.2 – Overview of final device concept

As will be discussed in section D, the short cavity plano-convex mini laser was not enough to enforce single mode operation due the wide gain bandwidth of over 100nm in the Cr:LiCAF or Cr:LiSAF laser materials. Thus we needed an additional mechanism to reinforce single mode selection, which we implemented in the form of a narrow band dielectric selection filter deposited directly onto the crystal.

Figure B.2 shows the schematic of the single-frequency final mini-laser for the wavelength range 750 nm and 850 nm that we envision for the PINS program. A 2mm Cr:LICAF, or Cr:LISAF crystal is placed under a slight angle between a concave and flat mirror forming a cavity for the laser mode at 780 or 850 nm. One side of the crystal is AR coated and on the other side the narrow band optical filter is deposited that enforces single-frequency operation of the laser. Only the frequencies transmitted through the filter see the curved mirror and therefore can form a stable cavity mode. All the other frequencies rejected by the filter only experience the flat-flat cavity and therefore no

stable cavity mode can form for those frequencies. In addition, due to the angle the flat surfaces are misaligned. These mechanisms enforce very strongly the single-frequency operation of the laser despite the presence of strong spatial hole burning [2, 3].

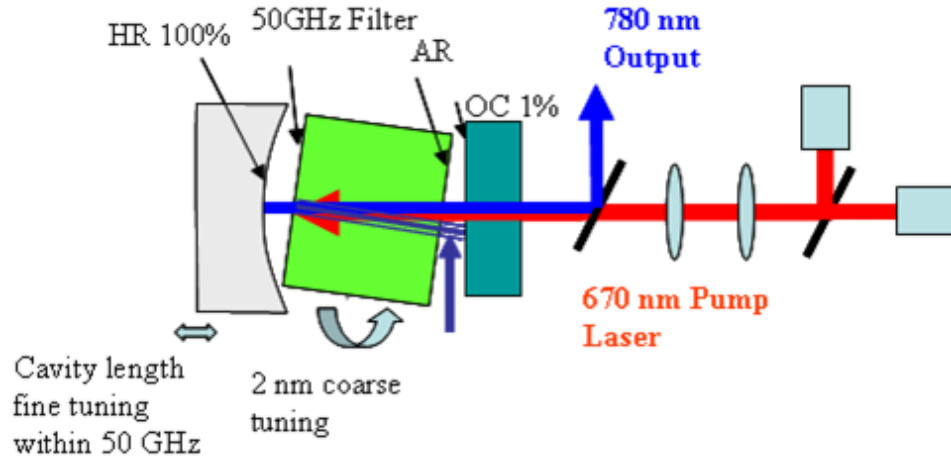


**Figure B.2:** Schematic layout of the single-frequency mini laser.

The crystal is under a slight angle varying between  $1^\circ$  and  $5^\circ$  so that the multi-layer filter can be angle tuned over a range of 2nm. The laser is directly diode-pumped with either a single or a pair of polarization multiplexed 670 nm laser diodes and if necessary it could be even extended to four diodes if pumped from both sides. The flat end mirror of the cavity is currently used as the output coupler. Later it could be formed by a semiconductor wafer that serves as a substrate to carry the output coupler and also as a tuning element for the fine tuning of the laser frequency by modulating the index of the semiconductor layer via heating or optical carrier injection. Additional cavity tuning can be achieved by mounting the curved mirror on a PZT.

### **B.3 – Semiconductor device for tuning, frequency modulation and locking**

Slow tuning of the laser can be achieved by angle tuning of the filter, i.e. the crystal. For a change in angle between  $1^\circ$  and  $5^\circ$  the filter transmission tunes over a range of 2nm. For fast tuning with speeds eventually up to 1 GHz we want to explore the use of optical

carrier injection in semiconductors, see also section D.5. Two possible layouts for such a device are shown in Figure B3 (a) and (b).

The coarse tuning of the single-frequency radiation to a selected wavelength can be achieved by temperature tuning of the semiconductor wafer (see section ??). For example the index of the GaP wafer shown in Figure B3 (a), which is 300  $\mu\text{m}$  thick shows a temperature dependent index change of  $\Delta n = 2 \cdot 10^{-4}/\text{K}$ . The thermally induced

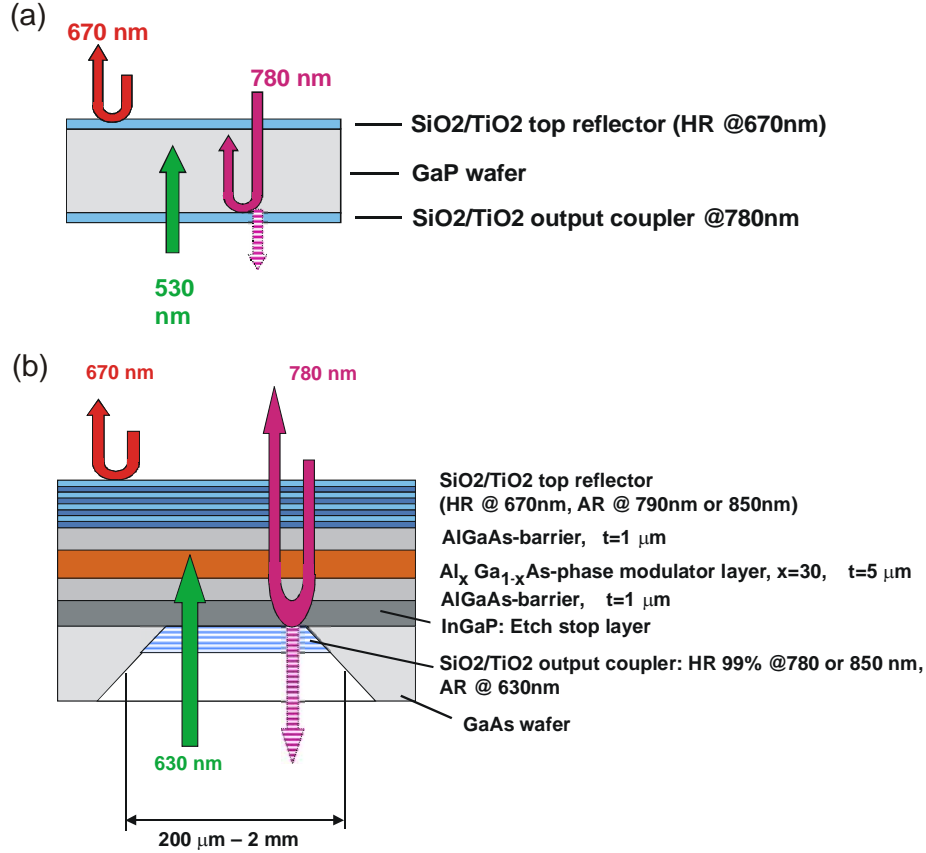


**Figure B3:** Semiconductor devices for fast and slow tuning of the mini laser: a) GaP-based device, (b) AlGaAs-based device.

phase shift in the GaP wafer leads to a temperature dependent frequency shift of the laser cavity of  $\Delta f = 75 \text{GHz}/\text{K}$ . Thus with a 1K temperature change we can tune the laser over two FSRs of the cavity including the semiconductor wafer, i.e. 30 GHz. Note, by choosing the thickness of the semiconductor layer we can easily change the sensitivity of the laser frequency to a temperature rise over as much as three orders of magnitude. For example in the device in Figure B3 (b) the laser beam experiences only the refractive

index change in the 5  $\mu\text{m}$  thick  $\text{Al}_x\text{Ga}_{1-x}\text{As}$  layer, which reduces the sensitivity by a factor of 60 to  $\Delta f = 1.2\text{GHz}/K$ . Also, the speed of the thermal modulation depends on the thermal design of the structure and is expected to vary from 50 Hz, for example for the 300  $\mu\text{m}$  thick GaP wafer of Figure B3 (a) to 5kHz for the structure in Figure B3 (b).

Thus, the thermal effect can be used for large but slow tuning.

The refractive index of semiconductors is not only strongly temperature-dependent but also dependent on carrier density via the plasma effect. For III-V semiconductors the index change as a function of carrier density is given by

$$\frac{\partial n}{\partial n_c} = -5 \cdot 10^{-22} \text{cm}^3 \quad (1)$$

These carriers can be generated optically, for example in GaP with a green laser or a blue laser diode with a wavelength shorter than 530nm. To shift the resonance frequency of the laser with the GaP wafer by 160 MHz, we only need an index change of  $\Delta n = 2 \cdot 10^{-6}$ . The necessary carrier density variation to achieve this index change is  $n_c = 4 \cdot 10^{15} \text{cm}^{-3}$ . If the carrier lifetime is assumed to be on the order of 10 nanoseconds, such a carrier density can be generated in a volume element with 50  $\mu\text{m}$  radius and 300  $\mu\text{m}$  length by only 18 mW of laser power. Such lasers are readily available even in the green/blue wavelength range, where GaP is absorbing. During Phase I we have investigated the phase change induced by optical carrier injection and those results are stated in section D.4. So observed index change is about a factor of 100 smaller than expected and we modulated with up to 3W of power to see a fast index change that corresponds to a frequency shift of 80 MHz. One reason might be the smaller carrier lifetime. Further investigations for this discrepancy, especially the measurements of the carrier lifetime will be performed using pump probe measurements.

In the low frequency range the index change will always be dominated by the thermal effects and therefore a detailed analysis of the device parameters is very important. Most critical is the carrier-lifetime in determining the strength of the carrier induced index change, which is usually not specified by any group or company that does the semiconductor growth. Also at wavelengths longer than 630nm very powerful laser



diodes are available for the carrier generation. It is for that reason that we presented different structures in Figure B3. Figure B3 (b) shows a semiconductor device, where we could use a diode laser at 630nm for the thermal and carrier modulation. Experimental characterization of the devices will be necessary to determine which one is the most suitable for our applications.

In the future we hope to design and characterize and optimize the semiconductor device for slow and fast tuning. The laser can be slowly tuned within the mode hop free tuning range by the thermal index change in the semiconductor wafer/layer. In addition, fast tuning of more than 150 MHz within 10  $\mu$ s as requested for the PINS project will be pursued by carrier-injection and as a back-up also by PZT's.

## **C. Multimode operation**

Through several iterations we have greatly improved the performance of our mini laser in multimode operation by matching the spatial overlap of the cavity mode and pump power, and by employing higher power n-Light pump diodes that have recently become available. Ultimately we achieved an optimized laser design with output power of up to 300mW for 1.5W pump power with a 37mW threshold value and low internal losses. An efficient multimode laser design is important for a single frequency laser and here we present progress we made on the multimode design.

### **C.1 – Preliminary multimode lasing results**

The initial cavity we built the cavity sketched in Fig. C1 (a), where actually the crystal should be AR-coated on both sides and the output coupler coating is on a separate substrate.

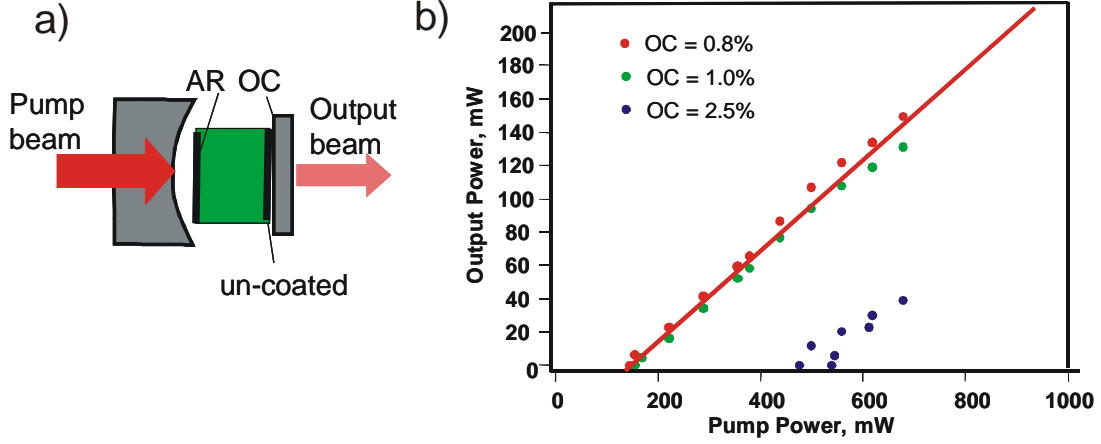


**Figure C.1:** a) Laser set-up; b) Experimentally demonstrated output power versus pump power characteristic of the laser for different output couplers. Radius of curvature of the curved mirrors was  $R = 30$  m.

However, due to difficulties with the company for polishing and coating the crystals, one surface in the laser of figure C1 (a) was not yet AR-coated, which leads to a reduction in the effective output coupling. Nevertheless, more than 150mW of output power could be demonstrated with about 700 mW of pump power. In these experiments the laser was still operating multimode, a typical spectrum is shown in Figure D3.

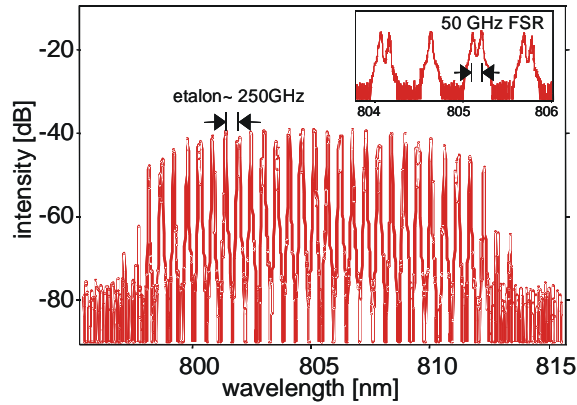


**Figure C.2:** Typical multimode output spectrum of the laser in Figure C1 (a).

Due to additional intracavity etalon effects caused by the uncoated crystal surface only about every 5th cavity mode with 250 GHz spacing is lasing corresponding to an intracavity etalon of 400  $\mu\text{m}$ .

## C.2 – Optimized output performance

In the subsequent iteration of the design, we have greatly improved the performance of the multimode operation in the Cr:LiCAF laser. The inset in Figure 2 indicates the cavity design for multimode operation. The cavity is a compact plano-convex cavity with a 1% output coupler. The pump light is directed through the output coupler which is transparent at 670nm, the pump wavelength. This was done since in single mode operation the filter, which doesn't transmit the pump wavelength, will be on the far side of the crystal. Also we have greatly increased the available pump power by switching to 1W n-Light pump diode lasers.

The Cr:LiCAF crystal is AR coated on one side and has a 37% coating on the other side from a previous design stage of the laser. Figure 1 shows the obtained multimode output power as a function of pump power. Pumping with two diodes up to 300mW output power was achieved with 1.5 W pump power. The 2mm long crystal absorbs about 60% of the pump power. A low laser threshold of only 37mW was achieved. These results indicate that we have optimized multimode operation and without additional losses in the single frequency selection process, we could potentially achieve up to 300mW output power in single frequency operation.

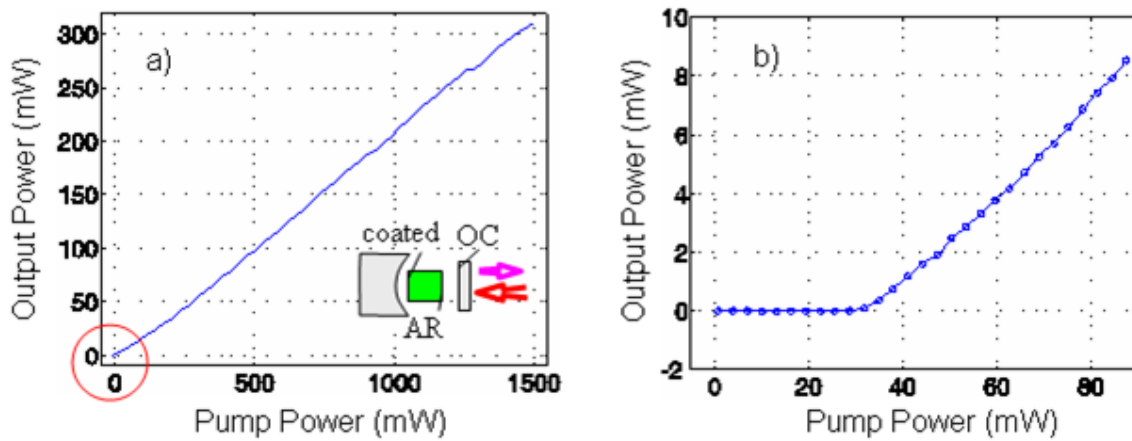


**Figure C.3:** (a) Output power versus pump power characteristic. The inset shows the schematic of the laser setup. (b) Zoomed in version indicates the low threshold of only 37mW. zoomed in portion of the full power trace near threshold. As indicated in the Figure the new laser design gives high output power and has very low threshold levels (37mW).

Also note that no thermal gain quenching was observed, so in principle higher output powers can be achieved by increasing the pump power even further. Since we have already used two polarization-multiplexed high power red diode lasers, more pump power could be achieved by using an additional pair of pump diodes, and pumping from the opposite side, however the narrow band filter would need to be modified to transmit the pump light.

### C.3 – Cavity losses

We also measured the losses for the nearly optimized cavity as indicated in Figure C.4. By measuring the output power verses pump power for a 1% and a 2% output coupler we see that the laser threshold value nearly doubles while the slope efficiency for high power remains nearly identical. This indicates that the losses in the overall system are dominated by the loss associated with the output coupling efficiency. Thus the intra cavity losses are much less than 1%. The optimized multimode laser performance for the Cr:LiCAF mini-laser is indicative of the potential this system has for single frequency operation.

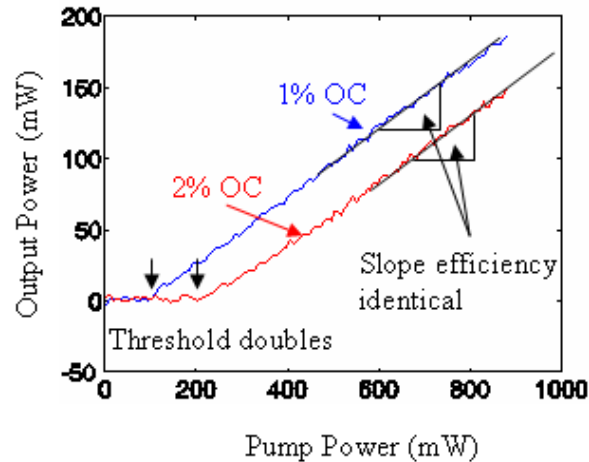


**Figure C.4:** The two curves above indicate that the intracavity losses are less than 1%

## **D. Single mode operation**

The high doping possible for the Cr:LICAF crystal, together with its high upperstate lifetime quenching temperature of 250°C, enables the construction of very short-cavity mini lasers of only 2mm length). Such short lasers already have a free spectral range (FSR) of about 0.1 nm corresponding to 50 GHz. However, the gain bandwidth of these crystals is on the order of 100 nm. Therefore, single mode operation must be enforced by additional frequency-selective elements.

In contrast to the initial plans in Phase I (see section D.1), we developed a narrowband filter to enforce single-frequency operation. This filter is directly deposited on the crystal so that there are no critical alignment steps for achieving single frequency operation. This greatly simplifies the construction of the laser in comparison to the initial design, because only the curved and flat mirror need to be aligned with each other, which is always automatically the case. Only the pump beam has to be aligned with the cavity mode. The alignment of the crystal only determines the laser wavelength but not the cavity stability. This is a significant improvement. Most importantly is the suppression of all undesired longitudinal modes because the cavity is unstable for all frequencies that do not pass through the filter, (see Fig. B1.) This avoids lasing at undesired frequencies which plagued us in the first version of the laser in Phase I.

In this section we present the initial air etalon concept and explain the difficulties we had with it, we present the final filter design and operation, and we report on the performance of the single frequency laser. We have achieved 20mW of single frequency power with a 5MHz linewidth. In addition we also present initial results on the tuning capabilities of the filter which indicate a 0.9nm tuning range and demonstrate significant index changes in GaP wafers by carrier injection, which can be used later for fast phase modulation in the laser potentially with GHz modulation speed

### **D.1 – Initial version**

We investigated several different filter and etalon combinations to enforce single-frequency operation and tunability over a 2nm wavelength range. To show the difficulty one runs into, we show here two versions. The version in Figure D.1 achieves single-

frequency operation by the combination of a 5nm wide filter deposited on the wedge that is also carrying the output coupler coating. This filter in combination with an air etalon selects a single longitudinal mode by high transmission. We characterized the tuning elements and it seems to work, however, inside the laser a beam reflected of from the filter under normal incidence built a stable cavity mode with the curved mirror and had enough overlap with the gain medium to start lasing before the actual desired laser mode could reach threshold.

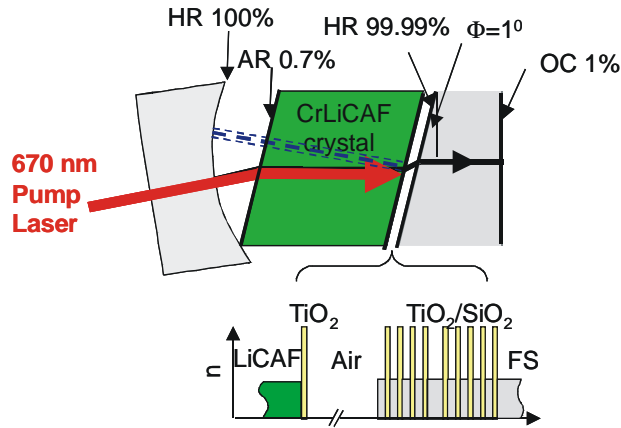


**Figure D.1:** Initial version of the tunable single-frequency mini laser.

## D.2 – Filter design and characterization

From this experience and the difficulty in aligning the laser crystal and the output coupler substrate to form a plan-parallel Fabry-Perot filter while still the laser cavity is aligned, we decided to go a different route, which is shown in figure D.2. The air etalon is avoided and instead the single-frequency operation is completely enforced by a narrow only one 1nm wide (FWHM) dielectric filter, which necessitates highest quality ion-beam sputtering with exceptional low scattering losses. Otherwise the width of the filter can not be maintained and most importantly the transmission losses become intolerably high (10%), which is unacceptable in our case. Note that this filter has a Finesse of about 1000 and a transmission loss of less than 0.5%.

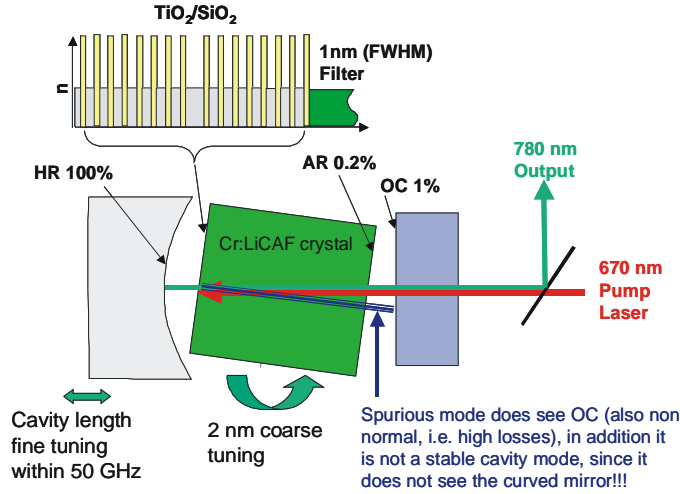


**Figure D.2:** Final version of the tunable single-frequency mini laser.

Since the filter is at the frontier of what current state of the art ion-beam sputtering technology can deliver, we did a test fabrication of this filter on a 2mm thick fused quartz substrate. A measurement of the transmission characteristic of this filter with a single-frequency diode laser is shown in Figure D.3. The diode laser was at a fixed wavelength and the filter was tuned by angle tuning. The Fabry-Perot fringes of the 2mm uncoated quartz substrate give a natural wavelength calibration. The spacing between the Fabry-Perot resonances is identical to the mode spacing in the mini-laser of about 50 GHz. Thus the FWHM of the filter of 1nm is about ten fringes wide, which is in perfect agreement with Figure D.3. Note, the transmission is significantly less than 99.5% because of the beam profile and divergence of the mode from the diode laser.

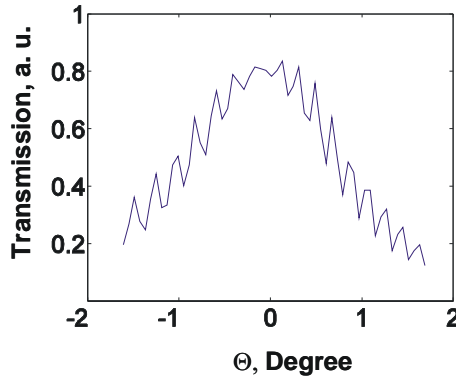


**Figure D.3:** Filter transmission measured with a single-frequency diode laser.

### **D.3 –Single mode operation:**

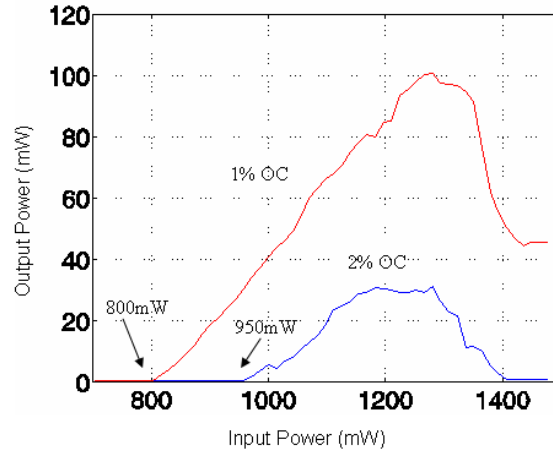
After the test fabrication we successfully had the filter design deposited directly onto the Cr:LiCAF crystal and implemented the mini laser shown in Figure D.2. Our initial assessment of the laser performance, measurement of intracavity loss, was done with the laser operating with only a few modes.

Figure D.4 shows the few mode (two or three) power behavior of the mini-laser configuration. The 1% and 2% output coupling curves indicate a 4% loss in the filter. A similar measurement for the multimode laser gave less than 1% loss, thus we know the 4% loss is from the dielectric filter. We have achieved an output power of 100mW close to the target value for few-mode operation despite the high losses from a first iteration filter design. These results can be further improved by reducing the filter loss by improving filter design and growth. The output power roll-off observed at high pump powers is due to the resonant cavity mode shifting of the transmission peak of the filter due to the thermal expansion of the crystal. This effect can be offset by simultaneous tuning of the cavity length.

With the setup shown in Figure D.2 a maximum output power of 20mW in stable single-frequency operation was obtained. Figure D.5(a) shows the optical spectrum in single frequency operation measured with an Advantest optical spectrum analyzer with 0.01nm resolution. The measured spectrum shows a 0.05 nm width limited by mechanical and thermal drifts of the cavity. Since the longitudinal cavity modes are separated by .076nm already this rough measurement confirms single-mode lasing. A higher resolution measurement was performed with a confocal scanning 1.5GHz Fabry-Perot cavity as shown in Figure D.5(b). The cavity was operated by adjusting the cavity length with a PZT by a length corresponding to a free spectral range of the cavity, 1.5GHz, and measuring the transmission with a photodiode. In the Figure the photodiode transmission and PZT drive voltage is plotted as a function of time. As indicated in the Figure, the two peaks correspond to the periodic transmission of the laser central wavelength, and the separation between the peaks is a free spectral range of the confocal cavity or 1.5GHz. If



there were other longitudinal modes lasing, additional peaks would appear over a single sweep range. Thus, the Fabry-Perot scan confirms that there is only one mode lasing.



**Figure D.4:** Output power versus pump power characteristics in few-mode operation with a 1% OC and a 2% OC. Roll over occurs due to the detuning of the filter from the laser mode position by thermal heating of the crystal.

We can use the output of the Fabry-Perot scan to coarsely evaluate the linewidth of the cavity. Figure D.6(a) shows a zoomed in region of the peak in Figure D.5(b) with the scale normalized to the free spectral range of the Fabry-Perot cavity. From Figure D.6(a)

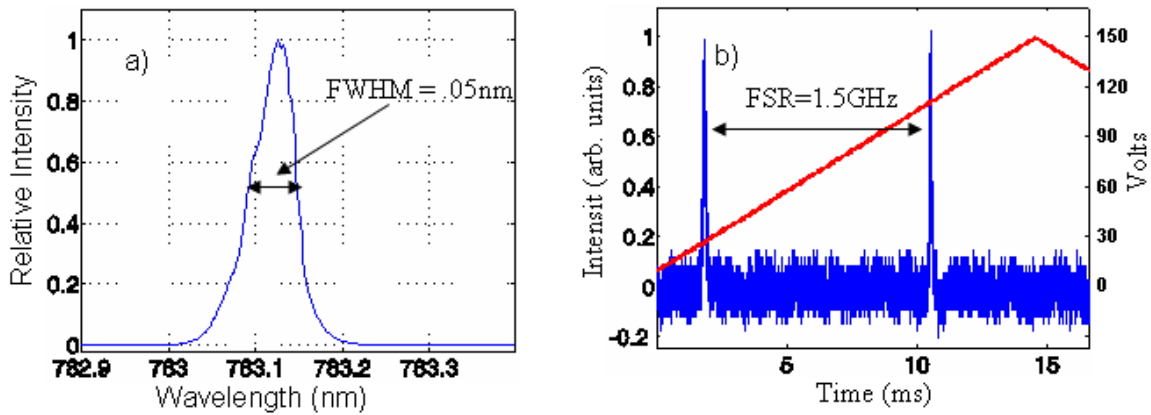


**Figure D.5:** (a) Optical spectrum of the single mode output limited by thermal drifting of the center frequency to 05nm. (b) Fabry-Perot scan of the single mode output indicates only one cavity mode is lasing. The triangle curve corresponds to PZT drive voltage (right axis), the curve with two peaks corresponds to the cavity transmission as measured with a photodiode (left axis).

we can estimate the linewidth to be better than 12MHz. Since the finesse of the cavity is 300, we can at best measure a linewidth of 5MHz, but since we are likely not optimally coupled into the Fabry-Pero cavity we can say that we are at the measurement limit of the Fabry-Pero cavity.

The linewidth of the laser was further characterized by beating the single-frequency solid-state laser output with the output from a single mode semiconductor diode laser with a 100kHz linewidth on a photodetector and analyzing the RF-spectrum. As

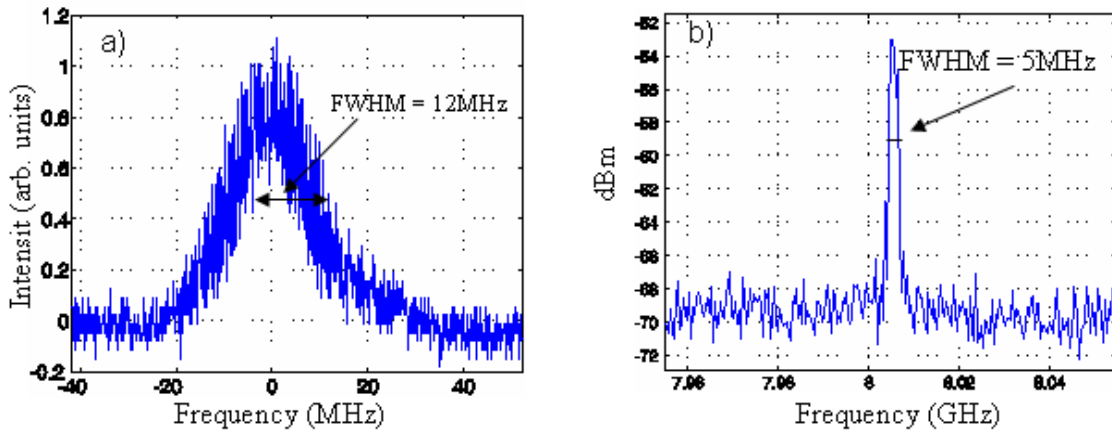


**Figure D.6:** (a) Rescaled Fabry-Perot scan of the laser output (from Fig D.5b). The width of the scan indicates a 12MHz linewidth. (b) Beat signal between the microchip laser and a 100kHz linewidth semiconductor diode laser. The best measurement of 5MHz (FWHM) was limited by the mechanical instability of the Cr:LiCAF laser.

shown in Figure D.6(b), a linewidth better than 5MHz (FWHM) could be measured using a 100kHz resolution bandwidth setting. Note that this linewidth corresponds already to the limit to be expected due to the passive stability of the simple laser cavity over the scanning period of the spectrum analyzer.

#### D.4 – Cavity mechanics

The mini laser is not surprisingly extremely sensitive to mechanical instabilities. Since the cavity length is extremely short (approximately 3mm), mechanical vibrations are more likely to drive the laser into relaxation oscillations. The initial mechanical configuration involved mounting the three laser components (curved mirror, crystal, and output coupler) to three separate 6-axis mounts. The added height and complexity

contributed to a mechanically unstable setup. In particular, the laser with the non-ideal mechanics was highly unstable and had large relaxation oscillations.

True single mode operation was only achieved when the mechanicals of the system was adequately stable. The final mechanics for the mini laser is shown in Figure D.7. The curved mirror, crystal, and output coupler are all mounted securely and with the minimum number of adjustments to an invar block.

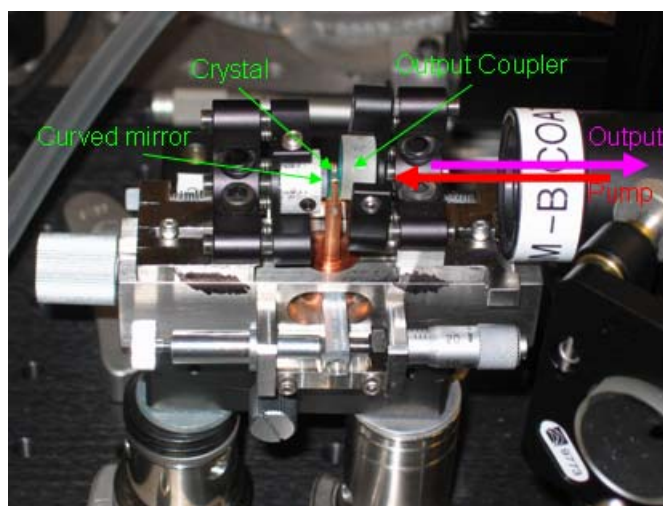


**Figure D.7:** Final mechanically stable mini laser setup. The filter is on the side of the crystal facing the curved mirror.

The output of this single frequency laser was put on a Si-photodetector and typical time traces are shown in Figure D.8. The output drifted slowly and at times is essentially flat for a few seconds. Aside from these slowly varying oscillations, the noise spectrum was essentially flat and the noise performance is best analyzed in terms of linewidth measurements as was done in the previous sections.

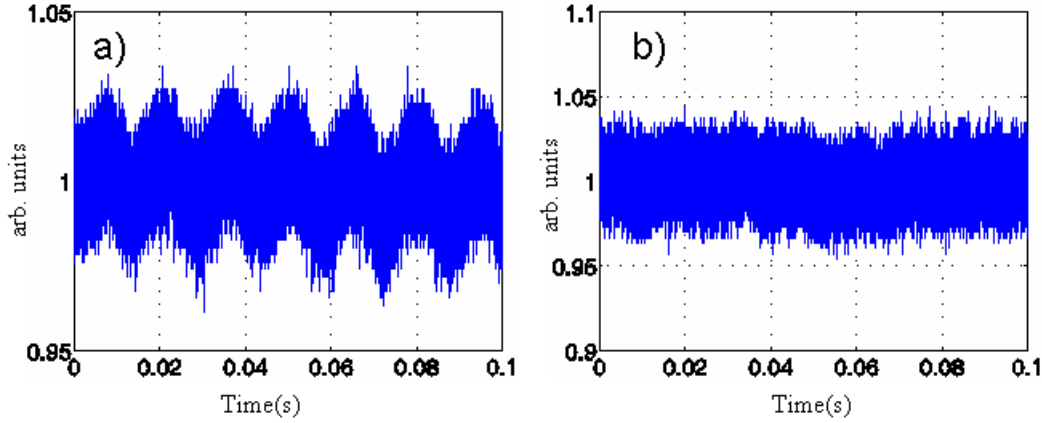


**Figure D.8:** Typical time traces of the single frequency output. The output slowly drifts between slowly oscillating (a) to stable (b).

We would also like to mention that we tried pressure fitting the laser components in a hollow aluminum cylinder with a spring loaded cap, see Figure E.1. This arrangement gave optimal stability in its single mode operation, and the laser output shined on a photodiode was essentially flat without the slow fluctuations observed in the Figure D.8. The lack of adjustments made it hard to optimize. In particular the cavity modes of the laser did not optimally overlap with the transmission of the filter. As a next step we would like to explore this design more carefully. Future mechanical designs will build off the cylinder concept by incorporating a PZT element to adjust the cavity mode frequency positions, and a mechanical flexure point to allow for fine angle tuning of the filter (see section E.1).

### **D.5 – Filter tunability: progress made in Ti:SAF**

We implemented the mini laser in a Ti:sapphire system as an intermediate step in developing the single frequency laser concept using angle tuning of the filter. The approach indicated in Figure D.2 was used with a few modifications. The crystal was Ti:sapphire and AR coated on both sides. The pump laser was a 532nm Verdi pump appropriate for pumping a Ti:sapphire crystal. Also, most importantly, the filter was a free standing filter coated on a thin glass plate which was AR coated on the opposite side.

Since Ti:sapphire has a shorter upperstate lifetime than Cr:LiCAF, the Ti:sapphire was insensitive to mechanical instabilities and so all four laser components (curved mirror, laser, filter, crystal, and output coupler) could be mounted and articulated independently in contrast to the mechanics needed for the Cr:LiCAF system, Figure D.7. Thus, by adjusting the filter angle by 2 or 3 degrees we were able to tune the lasing wavelength by 0.9nm or 450GHz as indicated in Figure D.9. The cavity was slightly longer due to the free standing filter and needed space for angle tuning so we could only operate the Ti:SAF mini laser with a few modes lasing. We expect to be able to extend these results to the Cr:LiCAF system.

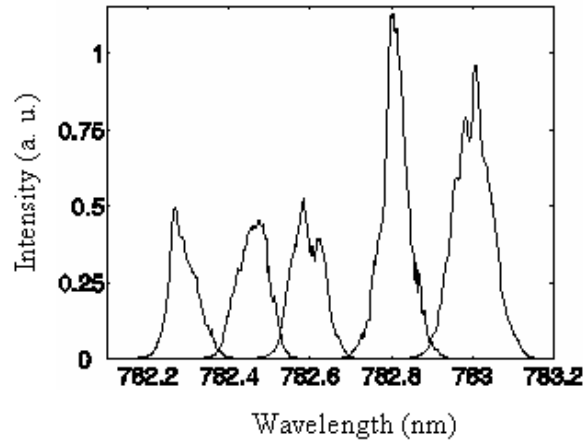


**Figure D.9:** Angle tuning of the mini Ti:sapphire system with the filter enabled frequency tuning of up to .9nm or 450GHz.

## D.6 – Tuning and modulation by carrier injection in semiconductors

Angle tuning of the laser crystal with the filter attached to it enables slow tuning of the laser over 2nm, if the angle is varied over about  $5^\circ$  as can be easily estimated from Figure D3; an angle of  $2^\circ$  corresponds to the FWHM of the filter of about 1nm. Fast tuning can be implemented by a PZT drive on one of the end mirrors of the mini-laser. However, a PZT can hardly tune faster than 100kHz, which barely meets the specifications of the PINS program. Therefore, we investigated an alternative fast tuning method based on the thermal index change in a semiconductor layer or the index change due to the electron

hole plasma in a semiconductor upon optical irradiation. The semiconductor material should be transparent to the laser wavelength of 780 nm and should be absorptive to the control light that generates the electron hole plasma. In the final laser this semiconductor material can serve as the substrate material for the output coupler of the laser and the device simply replaces the output coupler of the laser, see Fig. B.3(a). A semiconductor material transparent to the 780 nm light and fabricated in wafer form is GaP. To demonstrate the capabilities of such a device we irradiated a 300  $\mu\text{m}$  thick GaP wafer with 3W of 530 nm light which is absorbed in the wafer and measured the induced index changes and corresponding phase shifts, see Fig. D.10.

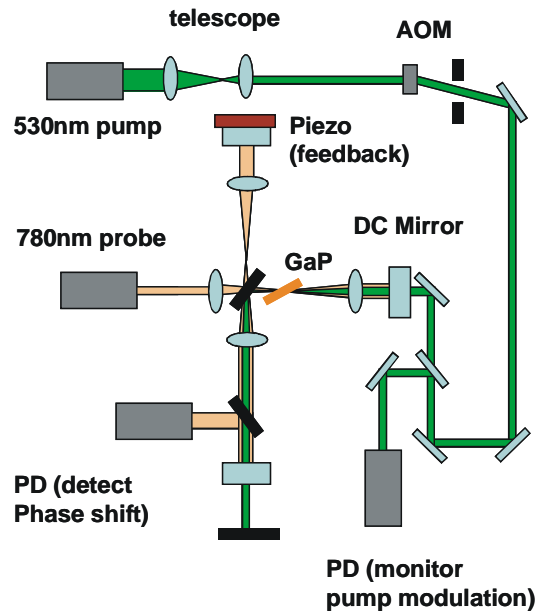


**Figure D.10:** Interferometric measurement of the index and phase changes in a GaP wafer due to the absorption of 3W of 530 nm light from a Coherent Verdi laser. The 530 nm light is modulated with an AOM. The index changes are monitored with a 780 nm diode. The interferometer is kept in quadrature by a low bandwidth (30Hz) feedback loop using a 670 nm control laser beam which is not shown in Figure D.10.

Figure D11 shows the measured calibrated phase shift as a function of modulation frequency.

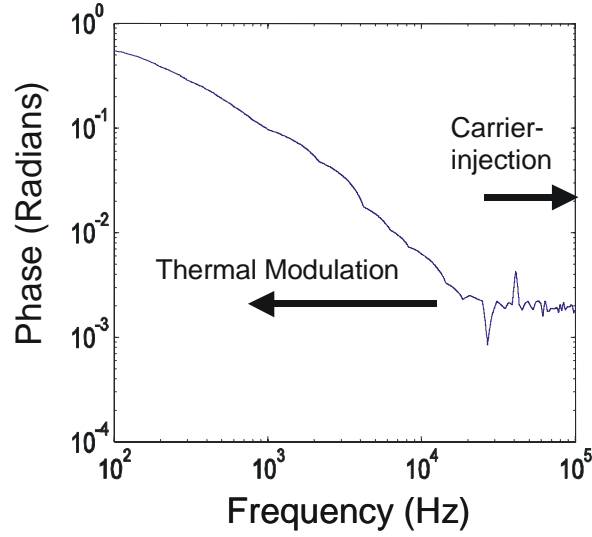


**Figure D.11:** Measured phase shift induced by 530 nm light as a function of modulation frequency.

From the spot size and thermal diffusivity of GaP we estimate a time constant for the thermal effects of about 3ms or a corner frequency of about 50Hz. The thermal effects are the reason for the large phase shifts at low frequencies up to 10kHz as can be seen in Figure D.11. For larger modulation frequencies the carrier induced phase shift dominates, i.e. the thermal effects are negligible. Currently we are limited to this frequency range due to the AOM. This study could be further extended to the GHz range with an EOM. In the presence of the multi-layer filter with a FWHM of 500 GHz, a phase shift of  $\Delta\phi$  leads roughly to a frequency shift of

$$\Delta f = \frac{500 \text{ GHz}}{2\pi} \Delta\phi. \quad (1)$$

Thus, even a phase shift of  $\Delta\phi = 10^{-3} \text{ rad}$  leads already to a frequency modulation of 80 MHz. This effect is supposed to be broadband, limited only by the lifetime of the carriers in the GaP wafer which is expected to be at most several nanoseconds. Exploiting the thermal effects which generate phase shifts on the order of 1 *rad* enables tuning over 80GHz, more than the longitudinal mode spacing. These experiments show that there is significant tuning possible by exploiting the thermal effects and the carrier-Plasma effects. However, the power consumption should be drastically reduced, since 3W of

optical power for tuning is too wasteful. Pump probe measurements should give the lifetime in the GaP-wafer. If the lifetime is too low, it might be advantageous to look into an AlGaAs based device such as shown in Fig. B3(b), where lifetimes on the order of 30 ns have been achieved.

#### **D.6 – Conclusion or why did we miss to deliver the Phase I milestones on time?**

When we started this project we were not aware how different the laser dynamics is for a single-frequency solid state laser with a long upper-state lifetime of 100  $\mu$ s and with a very short cavity compared to longer cavity single-frequency lasers. To understand that let's consider an example: The frequency tuning of a laser as function of the cavity length variations is

$$\frac{\Delta f}{f_0} = \frac{\Delta L}{L_0} \quad (2)$$

where  $f_0 = 400 \text{ THz}$  and  $L_0$  is the cavity length of the laser. For typical lasers with 10 cm or even 1 m cavity length and a mechanical thermal stability of 1  $\mu$ m this results typically in a frequency stability of  $\Delta f = 10^{-5} \dots 10^{-6} f_0 = 400 \text{ MHz} - 4 \text{ GHz}$ . In the here pursued 2 mm long mini-laser this sensitivity is two to three orders of magnitude larger. That means already 1 nm change make as much frequency drift, that is why the linewidth currently is in the MHz range, when measured fast enough and over long times it is even 25 GHz wide, or 0.05 nm as measured in Figure D.5(a) with the slowly scanning OSA. For this compact laser this corresponds only to a thermal drift of the cavity length by about 100 nm. Without active stabilization it is impossible to keep much higher mechanical precision over time. This is not only the origin of the currently large linewidth but this was also the reason for the relaxation oscillations of the laser, we were not able to understand for two months over the summer. The cavity vibrations shift the cavity modes significantly around and therefore the laser always stops lasing and starts from new, which leads to pronounced relaxation oscillations because of the long lifetime of the gain medium. Looking back with some distance on this project it was a big mistake to try to build the laser first with all discrete components rather than trying to build an



integrated laser immediately, because of the then much higher stability. This higher sensitivity is clearly a price we pay for the much more compact source. Since we understand these issues now, we think that we could still make this source meet the PINS requirements even with a very modest amount of funding. The different possibilities for further development are discussed in the next section.

## **E. Future possible work**

So far we achieved stable, single frequency operation with an output power of 20mW and a linewidth 5MHz. Although this is a significant first step, we have not reached the output power we expect. In multimode operation we were able to get up to 300mW. In the absence of any additional loss, we should get near the multimode power level. In section D.3 we estimated the losses in the filter to be 4%. Currently, this additional loss from the filter is limiting the output power of the system where single frequency operation occurs. In future design iterations, we will focus on reducing the filter losses..

We discuss in this section several ideas that could greatly improve the laser performance. First we discuss the stability limit of the setup and present a solution to approach the stability limit. Then we discuss improving the pump packaging. Next we present a graded filter for a widely tunable laser, and finally we present ideas of locking to compact ultra-low expansion cavities to achieve Hertz-linewidth levels.

### **E.1 Enhancing single-frequency stability and mechanical design**

We estimate here the unlocked linewidth limit for the mini laser. The crystal and laser mount can be kept at constant temperature by a thermo-electric cooler and a feedback control circuit. We can use SuperInvar mounts for the mechanics that hold the end-mirrors of the cavity. The coefficient of expansion is  $\Delta L_{\text{mech}}/L_{\text{mech}} = 0.6 \cdot 10^{-6} / K$  for SuperInvar. The optical expansion coefficient of the crystal is the sum of the mechanical expansion coefficient of LICA  $\Delta L/L = 3.6 \cdot 10^{-6} / K$  and the index change due to

temperature  $\Delta n/n = -4.2 \cdot 10^{-6} / K$  of LICAF, which is  $\Delta L_{\text{LICAF}}^{\text{opt}} / L_{\text{LICAF}}^{\text{opt}} = -0.6 \cdot 10^{-6} / K$ . This analysis shows that according to the published data for the materials discussed, the temperature dependence of the overall cavity, which is the optical length change due to the thermal effects of the cavity mounting and the thermal effects of the crystal, should balance out precisely. Most likely this will at best happen to the level of  $\Delta f/f = 10^{-7} / K$ . This analysis shows that the overall laser frequency should be very stable and temperature insensitive. In fact with a highly stable temperature control of  $\Delta T = 10^{-6} K$ , which is possible for a well isolated cavity, we should ideally get a direct absolute frequency stability of the laser to the level of  $\Delta f = 10^{-13} \cdot 400 THz = 40 Hz$ . This is the case without any tuning mechanisms attached and neglecting acoustic vibrations. Although the linewidth of our current setup is far from this level of stability, by improving the mechanical design we hope to approach these levels.

As mentioned in section D.4 we had great success with the compact SuperInvar mount shown in Figure D.7. We also discussed the pressure fitted mount shown in Figure E.1.

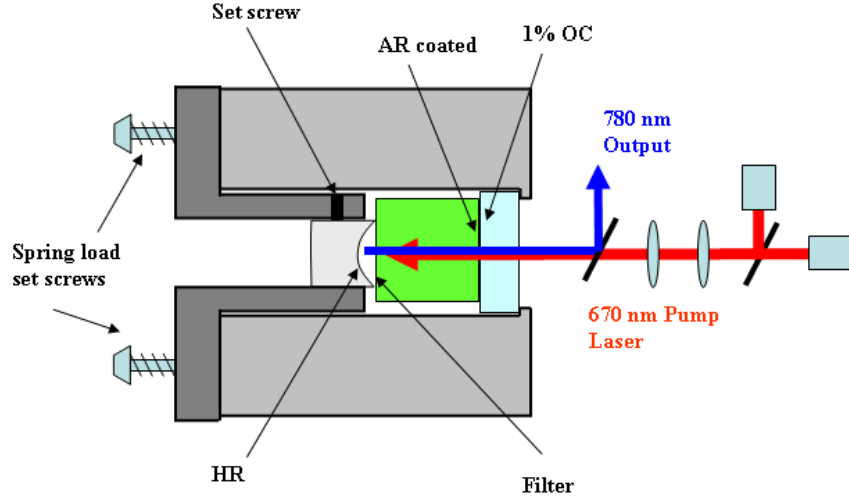


**Figure E.1:** Compact mechanically stable cylinder design.

Here we present a similar design with more adjustments, see Figure E.2. As shown in the figure, the PZT crystal can be used to ensure that a cavity mode is always aligned with

the transmission of the filter. The PZT can also be used to lock the laser. There is also a lever arm defined by the micrometer position and the notch indicated as the lever arm pivot in the figure. This configuration can be used to define an angle between the output coupler and the filter. Once this angle is defined, the cavity can be adjusted to maximize overlap between the cavity mode and the pump. The angle determines the transmission wavelength. Thus we are able to define the transmission wavelength and adjust the cavity modes to that wavelength in a compact mechanically stable configuration. We would like to pursue this design in future iterations of the mini laser.

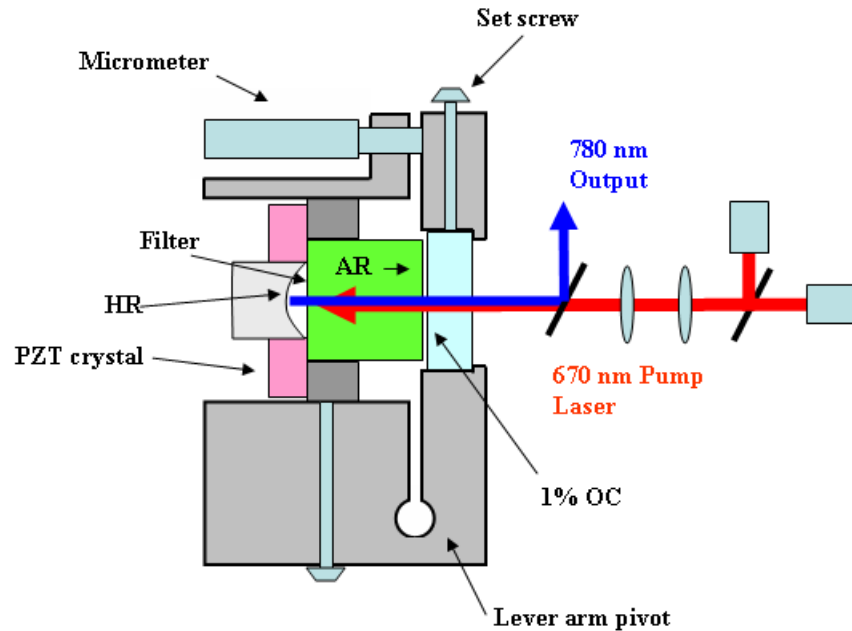


**Figure E.2:** Compact mechanics. The components are held together either with set screws (as indicated) or with thermally stable epoxy. The PZT allows one to adjust the cavity so that one cavity mode overlaps with the transmission of the filter. The micrometer and lever arm pivot allow a defined angle between the filter and OC which sets the transmission wavelength.

## E.2 Improving pump packaging

The development of a compact pump module, which could eventually be fiber coupled without losing too much in brightness, is an important step in developing a compact, stable SF laser. An example of such a module is shown in Figure E.3. Diodes with 500mW or 1W output power could be combined to make 1W and 2W pump modules without losing too much in brightness.

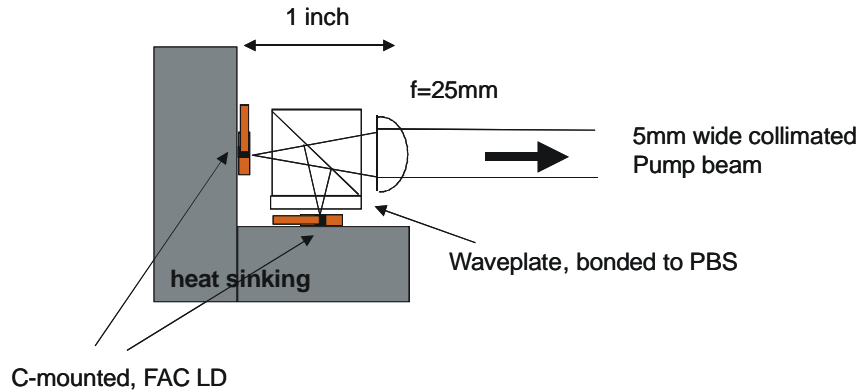


**Figure E.3:** Compact pump module based on two polarization multiplexed diodes. Diodes with 500mW and 1W output power are now commercially available and could be combined to make 1W and 2W pump modules.

The same overall concept discussed so far will be also applied for the construction of a single-frequency laser for the 850 nm range. We will again try Cr:LICAF as the active medium for this wavelength range, however, due to the reduced gain at 850 nm it might be necessary to switch to Cr:LISAF, which has its maximum gain at 850 nm.

### E.3 – Graded filter for widely tunable single-frequency laser

We would like to explore alternative approaches for single frequency selection with wide tunability. Instead of having a fixed filter attached to the crystal and using angle tuning. We could deposit the thin-film filter on a separate substrate of 1 mm thickness. The spacer layer determining the resonance wavelength of the filter can be grown in a graded fashion such that the layer thickness vary by 12% over a distance of 1cm, see Figure E.4. The laser can then be tuned over 100 nm by simply sliding the filter through the cavity. Various mechanisms shall be explored such that the tuning occurs without mode hopping. For example proportional to the tuning the cavity length can be varied with a PZT to avoid mode hopping.

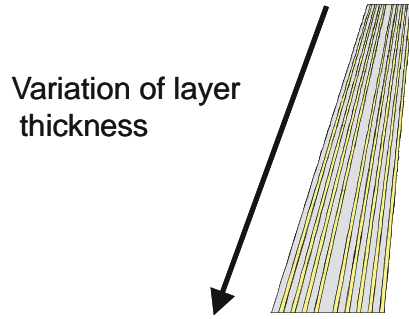


**Figure E.4:** Optical filter with spatially varying layer thicknesses. With a 12% gradient in layer thickness over 10 mm, 100 nm tunability can be realized.

#### E.4 – Compact ULE-cavities for Hertz-linewidth lasers

We would like to stabilize the output frequency to the sub-Hertz level by locking of the laser to ultra-low expansion cavities, [5]. These cavities are based on ultra-low expansion glasses having expansion coefficients of  $\Delta L/L = 10^{-8} / K$ . To reach Hertz level precision typically rubber band suspended meter long cavities using this material as spacer layers have been built. More recently a more compact cavity about 50 cm long that is balanced such that acoustic vibrations and gravitational forces do not deform the cavity has been used to demonstrate sub-Hertz linewidth lasers [6]. Here we want to pursue an approach

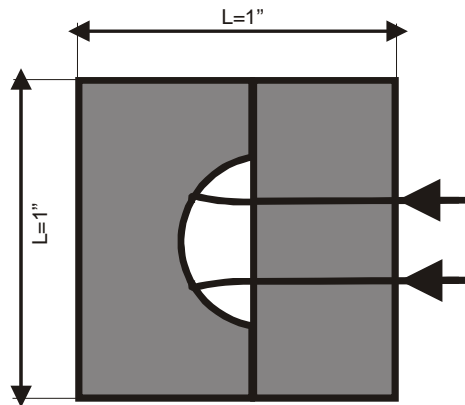


**Figure E.5:** Monolithic ULE-cavity with ultra-low loss ion beam-sputtered mirror coatings exhibiting a Finesse of  $10^5$ .

towards more miniaturized cavities. We would like to test the stability of very small ULE cavities that show narrow resonances by combining them with ultra-low loss mirrors, having reflectivities of 99.999% so that the overall resonance width is comparable to that of larger cavities. Figure B5 shows such a cavity, that is fully made from ULE material and the two mirrors are fusion-bonded together. This monolithic ULE cavity can then be placed in a vacuum vessel for temperature and acoustic isolation. Due to the small dimensions of the cavity, low frequency mechanical resonances can be avoided. Due to the low expansion coefficient together with proper thermal shielding the temperature drift can be made as small as 4 Hz if changes in the temperature are kept below 1  $\mu$ K. We like to investigate whether the fabricated single-frequency lasers can be locked to these cavities and what the resulting linewidth and stability will be.

## F. References

1. Schneider, K., et al., *1.1-W single-frequency 532-nm radiation by second-harmonic generation of a miniature Nd:YAG ring laser*. Opt. Lett., 1996. **21**: p. 1999-2001.
2. Zayhowski, J.J., *Limits imposed by spatial hole burning on the single-mode operation of standing-wave laser cavities*. Optics Letters, 1990. **15**: p. 431-433.
3. Kärtner, F.X., B. Braun, and U. Keller, *Continuous-wave-mode-locked solid-state lasers with enhanced spatial hole-burning, Part II: Theory*. Applied Physics B, 1995. **61**: p. 569-579.
4. Iseemann, A. and C. Fallnich, *High-Power Colquiriite Laser with high slope efficiencies pumped by broad-area laser diodes*. Optics Express, 2003. **11**: p. 259-264.
5. Young, B.C., et al., *Visible Lasers with Subhertz Linewidths*. Phys. Rev. Lett., 1999. **82**(19): p. 3802-3806.
6. Ye, J. in *Advanced Solid-State Photonics*. 2005. Vienna, Feb 6-9: OSA.
7. Conroy, R.S., et al. *Gain guiding and thermal distortion in diode-pumped Nd:YVO<sub>4</sub> microchip lasers*. Proceedings of CLEO 1996.